Electronic Supplementary Material (ESI) for Organic Chemistry Frontiers.
This journal is © the Partner Organisations 2022

Electronic Supporting Information

A π-Extended Phenanthrene-Fused Aza[7]helicenium as Novel Chiroptically-Active Architecture in Organic and Aqueous Media

Céline Olivier,*[a] Nao Nagatomo,[b] Tadashi Mori,[c] Nathan McClenaghan,[a] Gediminas Jonusauskas,[d] Brice Kauffmann,[e] Yutaka Kuwahara,[b] Makoto Takafuji,[b] Hirotaka Ihara[f] and Yann Ferrand*[g]

This PDF file includes:

1. Materials and Methods

1.1 Nuclear Magnetic Resonance and High-resolution Mass spectrometry analyses

NMR spectra were recorded on 2 different NMR spectrometers: (1) an Avance I NMR spectrometer (Bruker Biospin) with a vertical 7.05T narrow-bore/ultrashield magnet operating at 300 MHz for ^{1}H observation, and 75 MHz for ^{13}C observation by means of a 5-mm direct BBO H/X probe with Z gradient capabilities; (2) an Avance III NMR spectrometer (Bruker Biospin) with a vertical 16.45T narrow-bore/ultrashield magnet operating at 700 MHz for ^{1}H observation by means of a 5-mm TXI $^{1}H/^{13}C/^{15}N$ probe with Z gradient capabilities. Chemical shifts are reported in parts per million (ppm, δ) with tetramethylsilane as an internal standard. ^{1}H NMR splitting patterns with observed first-order coupling are designated as singlet (s), doublet (d), triplet (t), or quartet (q). Coupling constants (*J*) are reported in hertz. Data processing was performed with Topspin 3.5 software. Samples were not degassed. $CDCl_3$ from Aldrich was used after filtration through an alumina pad.

HR-MS spectra were performed by the CESAMO (Bordeaux, France) on a Q-exactive mass spectrometer (Thermo). The instrument is equipped with an ESI source and spectra were recorded in the negative/positive mode. The spray voltage was maintained at 3200 V and capillary temperature set at 320°C. Samples were introduced by injection through a 20 μL sample loop into a 300 μL/min flow of methanol from the LC pump.

1.2 Molecular modeling

Molecular Models calculation were performed using MacroModel version 8.6 (Schrödinger Inc.) with the Merck Molecular Force Field static (MMFFs) as implemented in this software. Energy minimized structures were obtained using 500 steps of Truncated Newton Conjugate Gradient (TNCG), chloroform as implicit solvent and the extended Cutoff option.

1.3 Crystallography

The diffraction data for compound rac-**1** were collected at the IECB X-ray facility (CNRS UMS 3033 – INSERM US001, University of Bordeaux) with a Rigaku FRX rotating anode (2.9 kW) diffractometer using CuKα wavelength with a partial chi goniometer (AFC11). The X-ray source is equipped with high flux Osmic Varimax mirrors and a Pixel-Hybride Dectris Eiger 1M detector. Data were processed with the Rigaku Oxford Diffraction CrysalisPro software (version1.171.40.69a).[1] The crystal structure was solved with Shelxt and refined by full-matrix least-squares method on F^2 with Shelxl-2014[2] within Olex2.[3] Non-H atoms were refined with anisotropic displacement parameters. H-atoms were refined in the riding-model approximation, with Uiso(H)=1.2Ueq (CH, CH2, NH). RIGU restraints were apply to model geometry of the molecules and thermal motion parameters. The asymmetric unit contains 4 molecules positively charged on the nitrogen atoms and 4 $PF6^-$ anions.

[1] CrysalisPro (Rigaku Oxford Diffraction, 2020).

[2] G.M. Sheldrick, *Acta Cryst.*, **2015**, *C71*, 3.

[3] O.V. Dolomanov, L.J. Bourhis, R.J. Gildea, J.A.K. Howard & H. Puschmann, *J. Appl. Cryst.*, **2009**, *42*, 339.

1.4 UV-visible absorption, Fluorescence emission, Electronic Circular Dichroism (ECD) and Circularly Polarized Luminescence (CPL)

UV-visible absorption spectra were recorded on a UV-1650PC JASCO spectrophotometer using a 1 cm pathlength quartz cuvette.

Steady-state emission spectra were recorded on a spectrofluorometer fitted with a PMT detector and exciting with a 450W Xe-lamp across a double monochromator, and were corrected for instrumental response. The fluorescence and reaction quantum yield were determined in degassed dichloromethane and air-equilibrated solutions as follows. The luminescence quantum yield (Φ) was calculated by using the equation $\Phi = \Phi_r(I/I_r)(A_r/A)(\eta^2/\eta_r^2)$ in which Φ_r refers to the quantum yield reference, I is the integrated emission intensity, A is the absorbance at the excitation wavelength and η is the refractive index of the solvent. An optically dilute solution of $Ru(bpy)_3^{2+}$ (λ_{exc} = 470 nm) was used as the standard (Φ_f = 0.018 in aerated CH_3CN). [4]

CD spectra were recorded on a JASCO J-815 spectropolarimeter using a 1 mm pathlength quartz cuvette.

CPL spectra were recorded on a CPL-300 spectrophotometer using a 1 cm pathlength quartz cuvette.

[4] H. Ishida, S. Tobita, Y. Hasegawa, R. Katoh, K. Nozaki, *Coord. Chem. Rev.* **2010**, *254*, 2449.

2. Molecular modeling

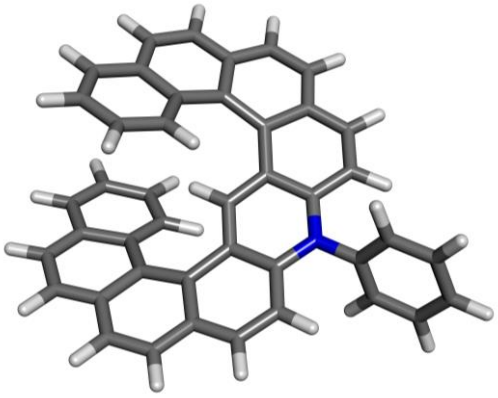

Figure S1. Model of targeted aza[9]helicene obtained by minimization using MMFFs.

3. Nuclear Magnetic Resonance

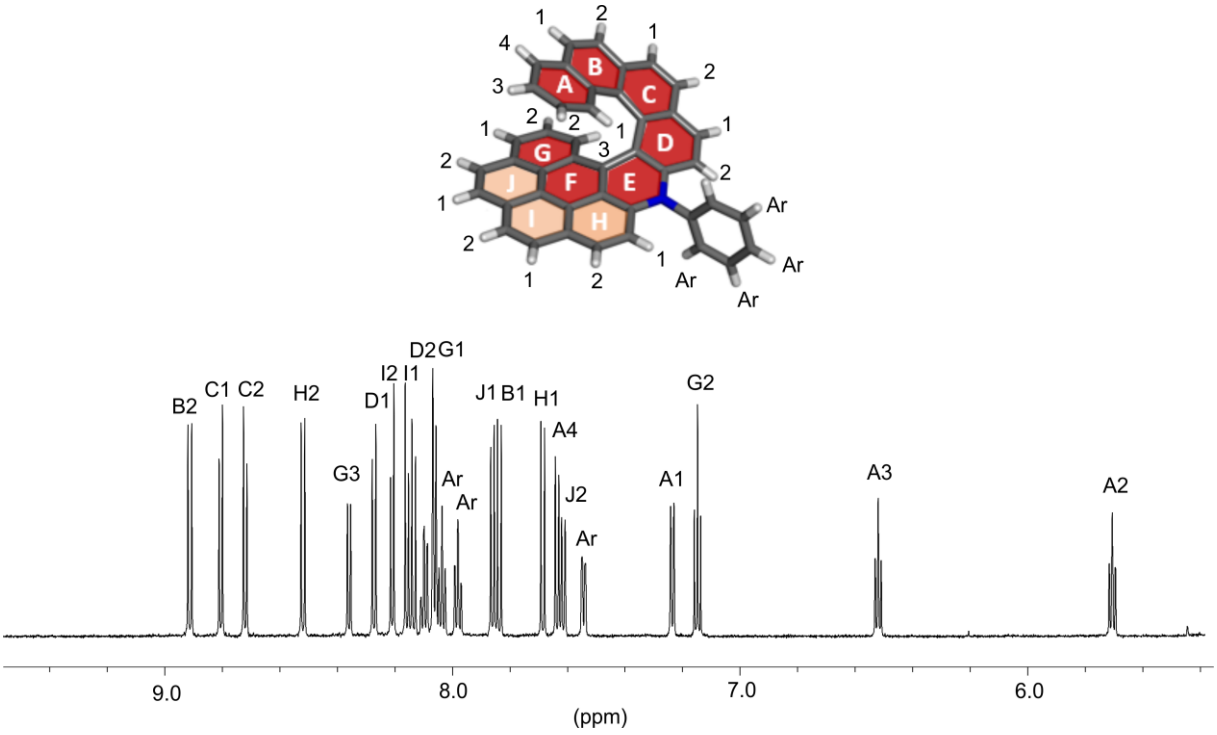

Figure S2. ^{1}H NMR (700 MHz, 298K) of rac-**1** in CD_2Cl_2.

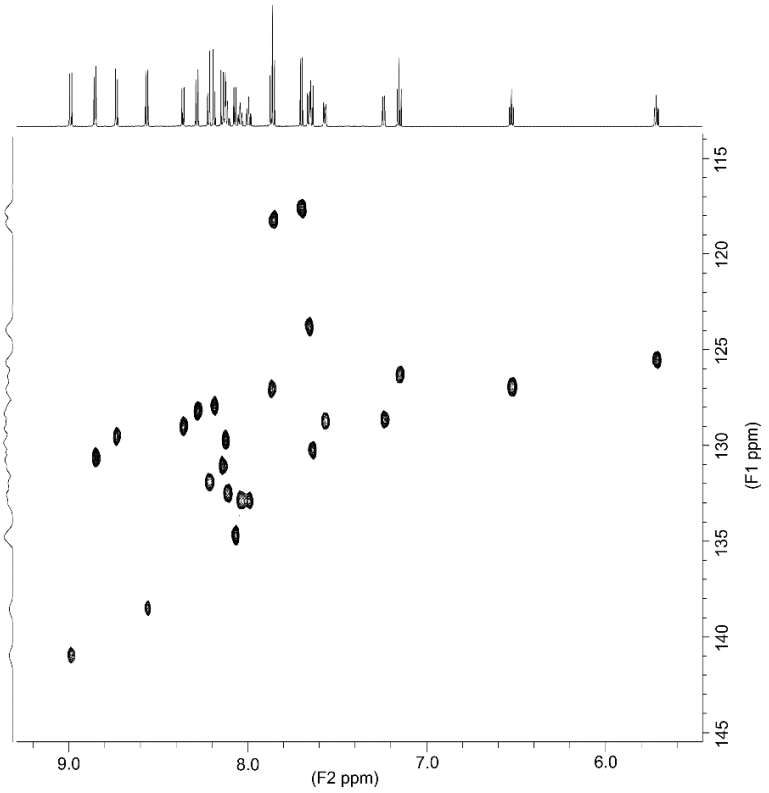

Figure S3. Part of the 700 MHz ^{1}H-^{13}C HSQC plot of rac-**1** in CD_2Cl_2 at 298 K, showing cross-peaks between directly bonded hydrogen and carbons. The horizontal scale is that of proton resonances and the vertical scale is that of carbon resonances.

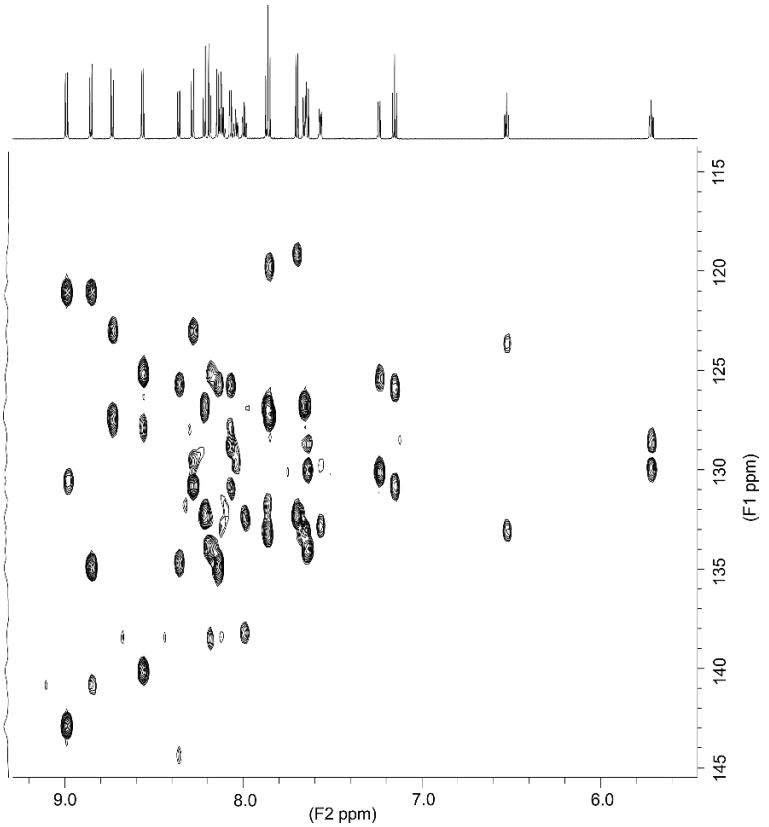

Figure S4. Part of the 700 MHz ^{1}H-^{13}C HMBC plot of rac-**1** in CD_2Cl_2 at 298 K. The horizontal scale is that of proton resonances and the vertical scale is that of carbon resonances.

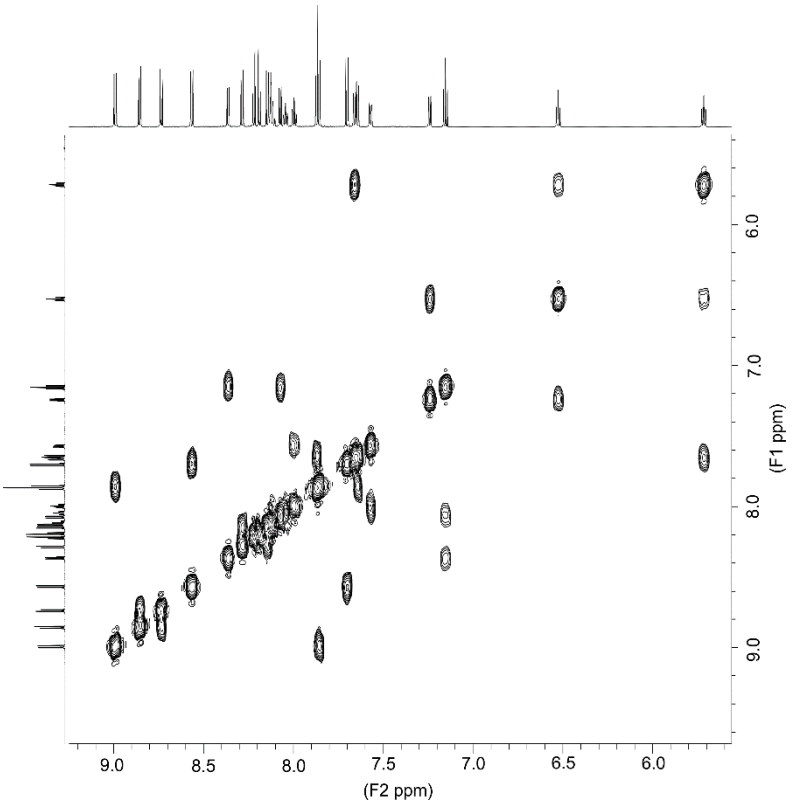

Figure S5. Part of the 700 MHz ^{1}H-^{1}H COSY of rac-**1** in CD_2Cl_2 at 298 K.

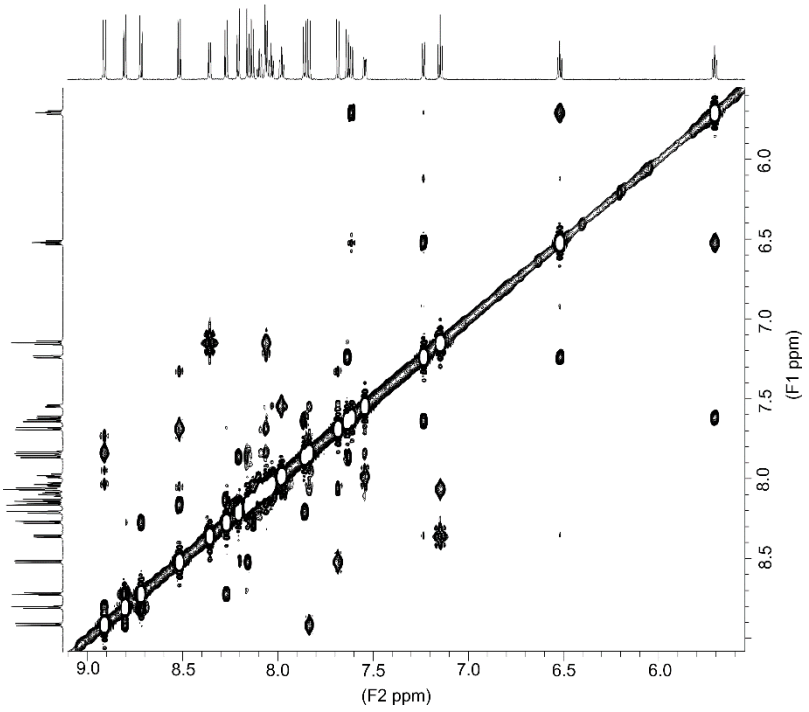

Figure S6. Part of the 700 MHz ^{1}H-^{1}H NOESY of rac-**1** in CD_2Cl_2 at 298 K (mixing time = 600 ms).

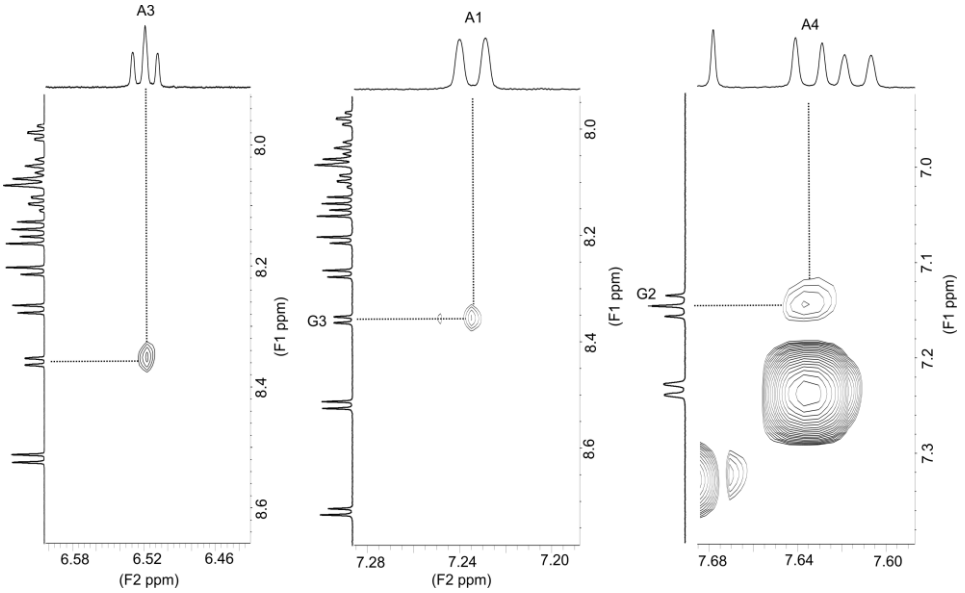

Figure S7. Zoom on the 700 MHz ^{1}H-^{1}H NOESY of rac-**1** in CD_2Cl_2 showing dipolar couplings between the terminal benzene rings A and G.

Table S1. Assignment of the ^{1}H and ^{13}C chemical shifts (ppm) for rac-**1** in CD_2Cl_2 at 298 K.

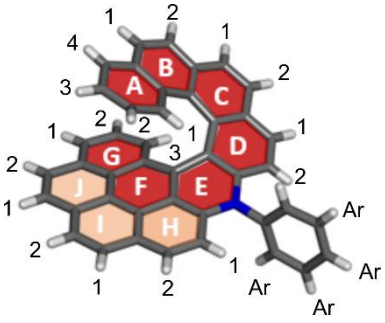

	^{1}H	^{13}C		^{1}H	^{13}C
A1	7.24 (d, 7.8 Hz)	128.6	**I1**	8.19 (d, 8.1 Hz)	127.9
A2	5.71 (td, 7.6 Hz)	125.3	**I2**	8.22 (d, 8.1 Hz)	131.9
A3	6.53 (td, 7.3 Hz)	126.8	**J1**	7.87 (d, 8.4 Hz)	126.9
A4	7.66 (d, 8.4 Hz)	123.6	**J2**	7.64 (d, 8.4 Hz)	130.2
B1	7.86 (d, 9.2 Hz)	118.2	**G1**	8.07 (dd, 7.8 Hz)	134.6
B2	8.99 (d, 9.2 Hz)	141.0	**G2**	7.15 (t, 7.8 Hz)	126.2
C1	8.85 (d, 8.2 Hz)	130.7	**G3**	8.36 (dd, 7.8 Hz)	129.0
C2	8.73 (d, 8.2 Hz)	129.5	**Ar**	7.56	128.7
D1	8.28 (d, 8.7 Hz)	128.2	**Ar**	7.99	132.9
D2	8.15 (d, 8.7 Hz)	131.0	**Ar**	8.04	132.8
H1	7.70 (d, 9.0 Hz)	117.6	**Ar**	8.11	132.5
H2	8.57 (d, 9.0 Hz)	138.5	**Ar**	8.12	129.7

4. Resolution by chiral HPLC

Instrumentation and method

Racemic compound **1** was analyzed with chiral HPLC system (JASCO Co., Tokyo, Japan), which consisted of a Gulliver PU-1580 intelligent HPLC pump with a Rheodyne sample injector (77251i), multi-wavelength UV detector (MD 1510 plus) and circular dichroism detector (CD-2095). Chiral separation was performed by using the CHIRALPAK® IA column (4.6 mm ø x 250 mm, DAICEL Co., Osaka, Japan). The typical chromatograms A and B (Figure S8) were obtained by a mixed mobile phase of chloroform, ethanol and trifluoroacetic acid (70 : 30: 0.01 in the volume ratio) at 0 ˚C and 0.5 mL min^{-1} in the flow rate.

The chiral resolution of **1** was performed with large diameter column of CHIRALPAK® IA column (10 mm f x 250 mm, DICEL Co., Osaka, Japan). As shown in Figure S9, the baseline separation was realized by 3 recycle processes, and then two portions (surrounded by a red dotted line) were collected and the solvents were removed. Finally, anion exchange using NH_4PF_6 (as described above) was performed to give *P*- and *M*- enantiomers of **1**, respectively.

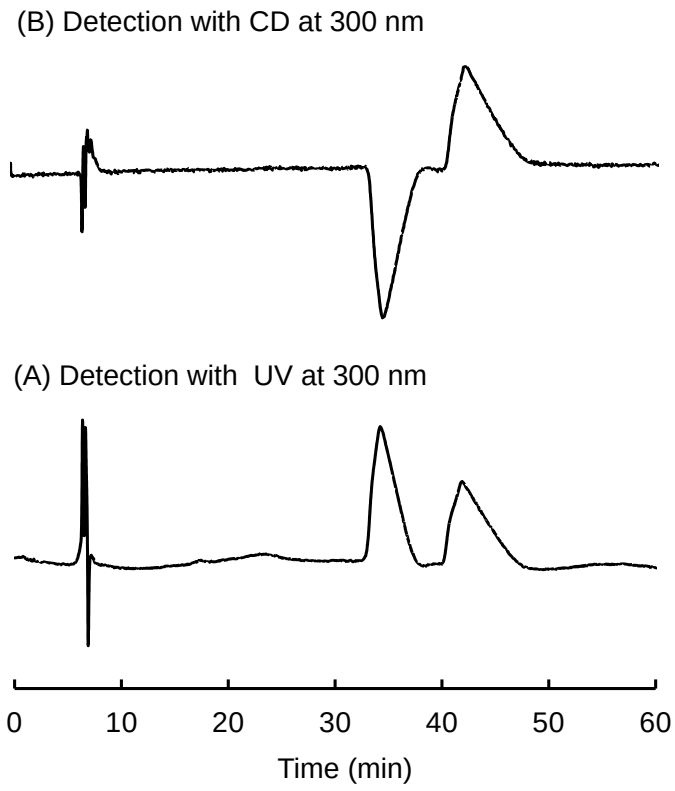

Figure S8. Chromatograms of rac-**1** obtained with CHIRALPAK® IA.

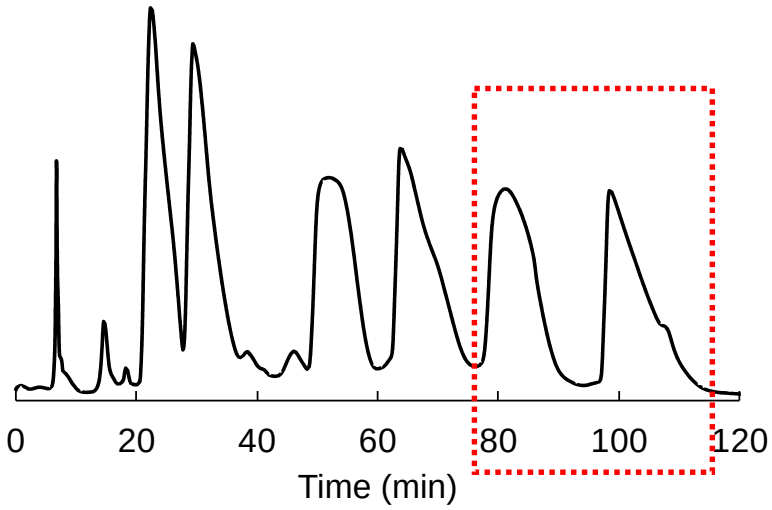

Figure S9. Baseline resolution of rac-**1** obtained with 3 cycle processes.

5. Opto-electronic studies of rac-1

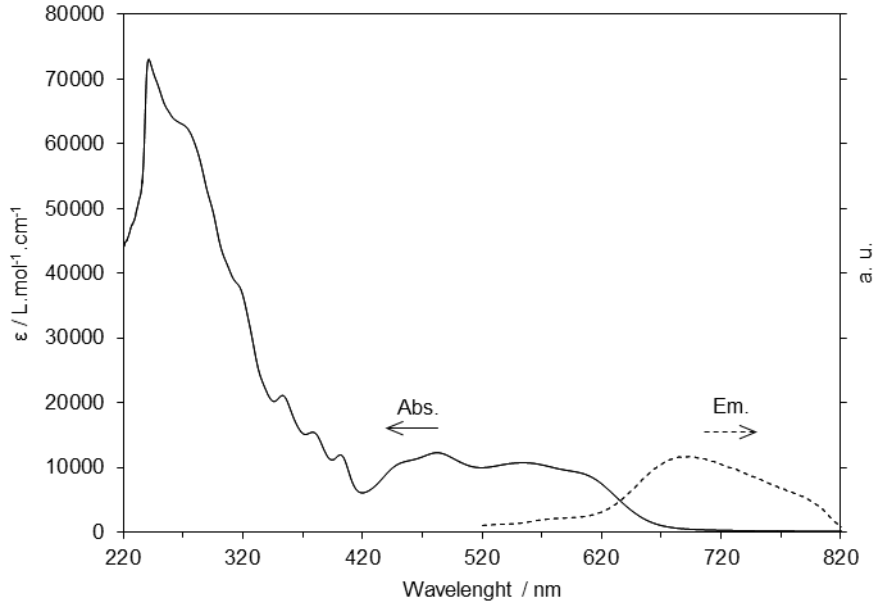

Figure S10. Electronic absorption (plain) and normalized fluorescence emission (dotted) spectra of rac-**1** in $CHCl_3$; C_{abs} = 20 µM ; λ_{exc} = 430 nm.

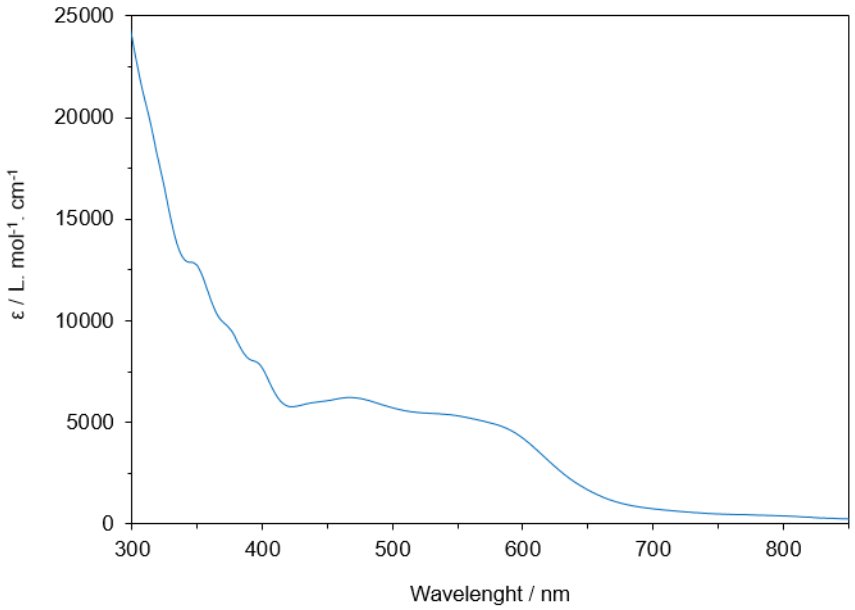

Figure S11. Electronic absorption spectrum of rac-**1** in H_2O-MeOH (9/1, v/v), C = 17 µM.

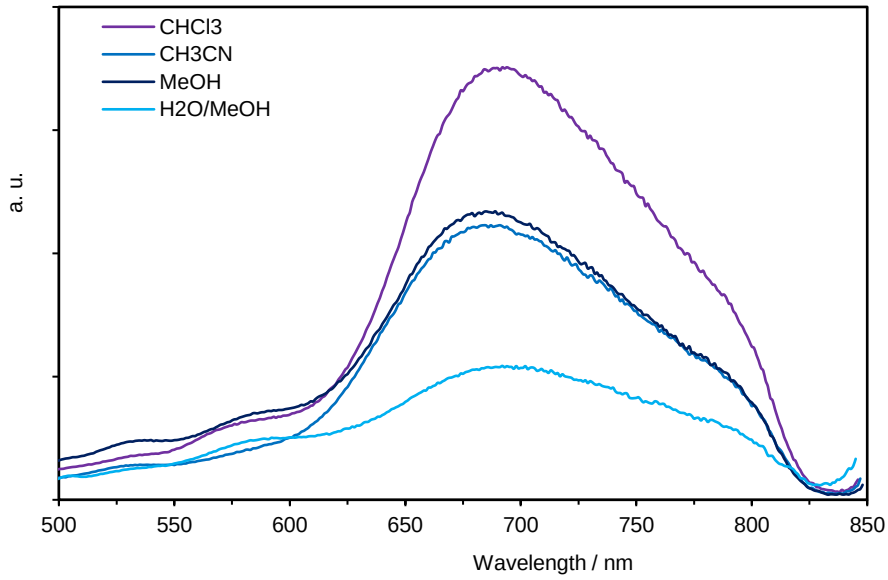

Figure S12. Fluorescence emission spectra of rac-**1** in different solvents: chloroform (purple), acetonitrile (navy blue), methanol (blue), water/methanol (9/1, v/v) (cyan). λ_{exc} = 430 nm

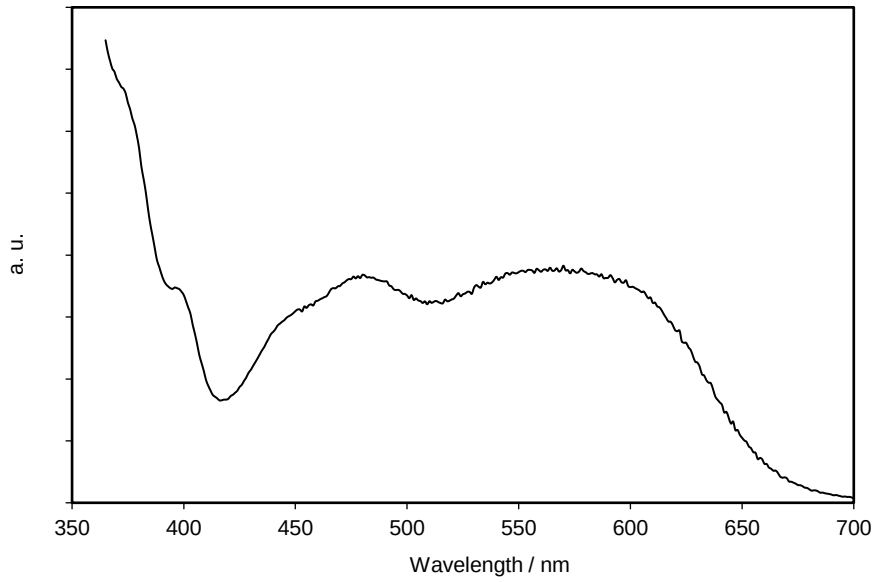

Figure S13. Excitation spectrum of rac-**1** in $CHCl_3$. λ_{em} = 700 nm

6. Chiroptical studies of *P*-1 and *M*-1 in aqueous medium

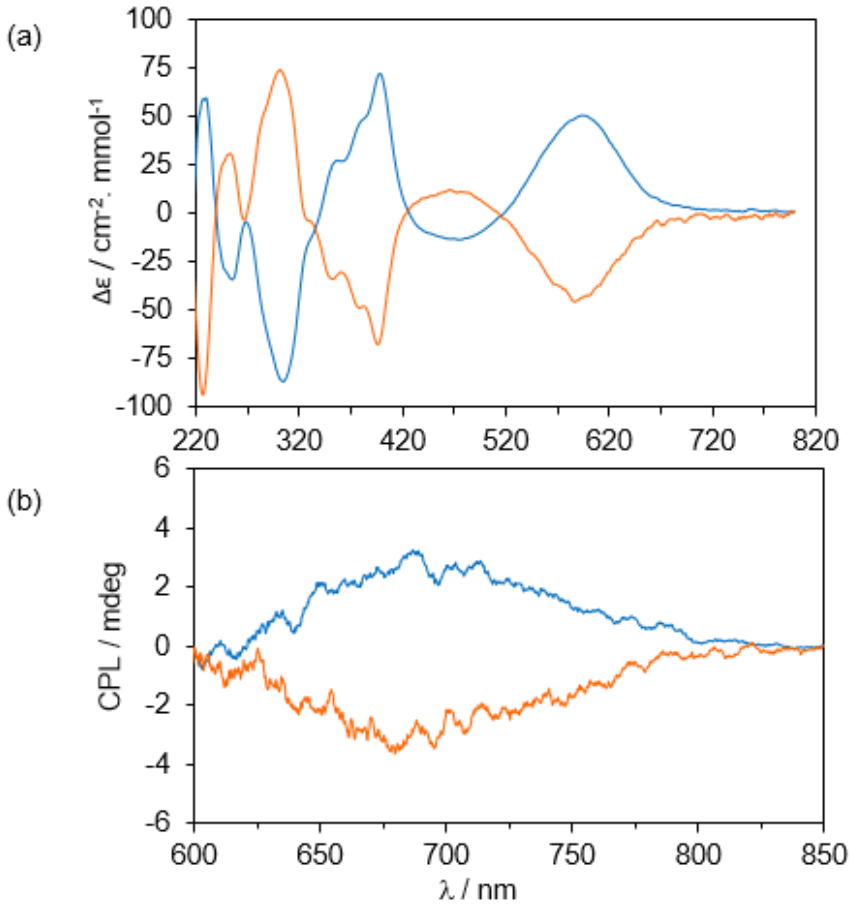

Figure S14. (a) ECD and (b) CPL spectra of the separated enantiomers of **1** recorded in H_2O/MeOH (9 :1, v/v). Cyan: first eluted peak (*P*-**1**); Orange: second eluted peak (*M*-**1**).

7. Theoretical calculations

All theoretical CD simulations were performed on Linux PCs by using the Turbomole 7.5 program suite.[5] The geometry of azahelicene was optimized at the TPSS/def2-TZVP level [6] with Grimme's 4th-generation dispersion correction.[7] The resolution of identity (RI) approximation was employed and the corresponding auxiliary basis-sets were taken from the Turbomole basis-set library. The numerical quadrature grid m5 was employed and the convergence criterion for the optimization regarding the change of total energy between two subsequent optimization cycles was set to 10^{-7} E_h. All excited-state calculations were performed with the above DFT optimized ground-state geometries, thus corresponding to the vertical transition approximation. The corresponding UV-vis and CD spectra were simulated by the RI-CC2 method using either def2-SVP or def2-SVPD basis-set. [8]The both basis-sets afforded the comparative results. For a direct comparison with the experimental spectra, the calculated rotational strengths of the latter in length gauge were expanded by Gaussian functions and overlapped where the width of the band at 1/e height is fixed at 0.4 eV.

Table S2. Summary of calculated transition in the visible region

Transition	eV	f	R	Configuration
1st	2.047	0.069	-222	HOMO → LUMO (90.3%)
2nd	2.269	0.048	43	HOMO-1 → LUMO (89.4%)
3rd	2.588	0.078	76	HOMO-2 → LUMO (88.2%)
4th	2.735	0.098	62	HOMO-3 → LUMO (89.1%)

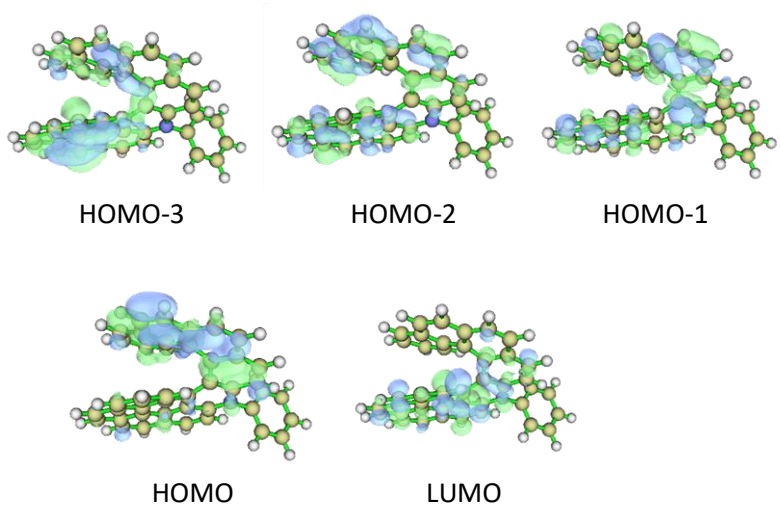

Figure S15. Relevant Molecular Orbitals of rac-**1**.

[5] S. G. Balasubramani *et al.*, *J. Chem. Phys.* **2020**, *152*, 184107.

[6] J. Tao, J. P. Perdew, V. N. Staroverov, G. E. Scuseria, *Phys. Rev. Lett.* **2003**, *91*, 146401.

[7] E. Caldeweyher, S. Ehlert, A. Hansen, H. Neugebauer, S. Spicher, C. Bannwarth, S. Grimme, *J. Chem. Phys.* **2019**, *150*, 154122.

[8] C. Hättig, A. Köhn, *J. Chem. Phys.* **2002**, *117*, 6939.

Optimized Geometry

Energy = -1708.770189016 (hartree)

C	0.0279354	-0.0463203	-0.5591665
C	0.0449563	-3.7211961	-0.0284353
C	0.5024661	-2.3800386	-0.0699289
C	0.5298420	4.9961128	-1.2095528
C	0.9867559	2.6159660	-0.8371183
C	1.4109632	0.2286461	-0.4515584
C	1.4491654	3.9580788	-0.8692295
C	1.8941614	1.5646544	-0.5529505
C	2.3329236	-0.8222192	-0.1994594
C	2.8048308	-3.2089233	-0.1496224
C	2.8177621	4.2186710	-0.6035189
C	3.1507795	-3.7985081	1.0638178
C	3.2644135	1.8448668	-0.3341364
C	3.3517142	-3.6397429	-1.3552237
C	3.7014279	3.1944092	-0.3544938
C	3.7108618	-0.5404205	-0.0417576
C	4.0678172	-4.8486899	1.0653153
C	4.1493844	0.7604997	-0.0898333
C	4.2674260	-4.6910368	-1.3418710
C	4.6243077	-5.2937178	-0.1347323
C	-0.3568536	2.3090996	-1.1769902
C	-0.4296720	-1.3075307	-0.0663267
C	-0.5786202	2.1466298	2.4134435
C	-0.7544327	4.7028663	-1.5702899
C	-0.8273356	0.9668675	-1.1328799
C	-0.9623575	0.9032427	1.9526762
C	-1.2279838	3.3533940	-1.5980887
C	-1.3002365	-3.9647742	0.0460104
C	-1.4825770	3.2257463	2.3870928
C	-1.7822480	-1.5820710	0.3663389
C	-2.0864568	0.6757523	-1.6804934
C	-2.2435682	-2.9204694	0.2558869
C	-2.2586284	0.6794777	1.4352030
C	-2.5132940	3.0221675	-2.0575946
C	-2.6818137	-0.5815965	0.8686964
C	-2.7838939	3.0122005	1.9839143
C	-2.9162533	1.6932193	-2.1404968
C	-3.2086417	1.7376460	1.5414195
C	-3.6348521	-3.1981530	0.3537538
C	-4.0725156	-0.8520553	0.7966863
C	-4.5255895	-2.1747323	0.5254424
C	-4.5851584	1.4744536	1.2699591
C	-5.0088923	0.2077842	0.9920306

N	1.8572005	-2.1105740	-0.1606503
H	0.4207714	2.2884751	2.8140658
H	0.7552174	-4.5352372	-0.0984776
H	0.8807334	6.0242045	-1.2092217
H	2.7086497	-3.4390152	1.9878992
H	3.0620871	-3.1600109	-2.2849872
H	3.1672472	5.2471546	-0.6215015
H	4.3474368	-5.3167232	2.0038291
H	4.4067184	-1.3510544	0.1361971
H	4.6997617	-5.0388432	-2.2746875
H	4.7498878	3.4092391	-0.1673492
H	5.2041564	0.9719830	0.0634118
H	5.3377705	-6.1117342	-0.1291100
H	-0.2652906	0.0761670	2.0168419
H	-1.1688802	4.2064998	2.7310598
H	-1.4377518	5.4960569	-1.8610857
H	-1.6642096	-4.9872781	-0.0030027
H	-2.4136092	-0.3541627	-1.7537264
H	-3.1793414	3.8163233	-2.3841140
H	-3.5142330	3.8157039	2.0316110
H	-3.8866546	1.4454384	-2.5581526
H	-3.9740326	-4.2244514	0.2471175
H	-5.2987125	2.2888691	1.3623036
H	-5.5953847	-2.3638170	0.5117061
H	-6.0675580	-0.0134695	0.8880851

8. X-ray crystallography

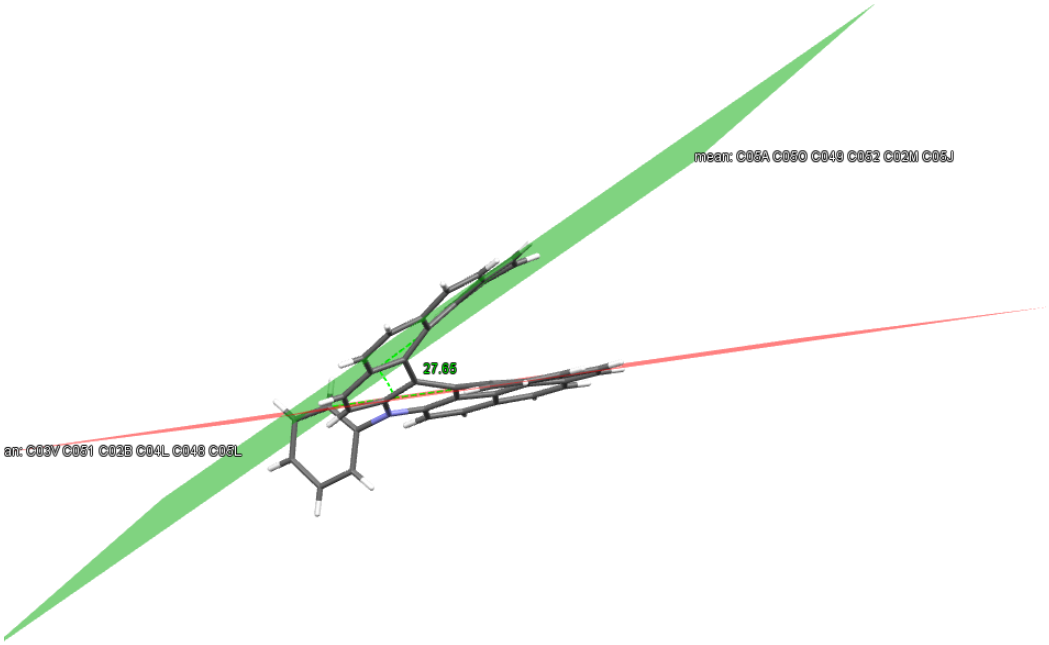

Figure S16. X-ray crystal structure of rac-**1**.

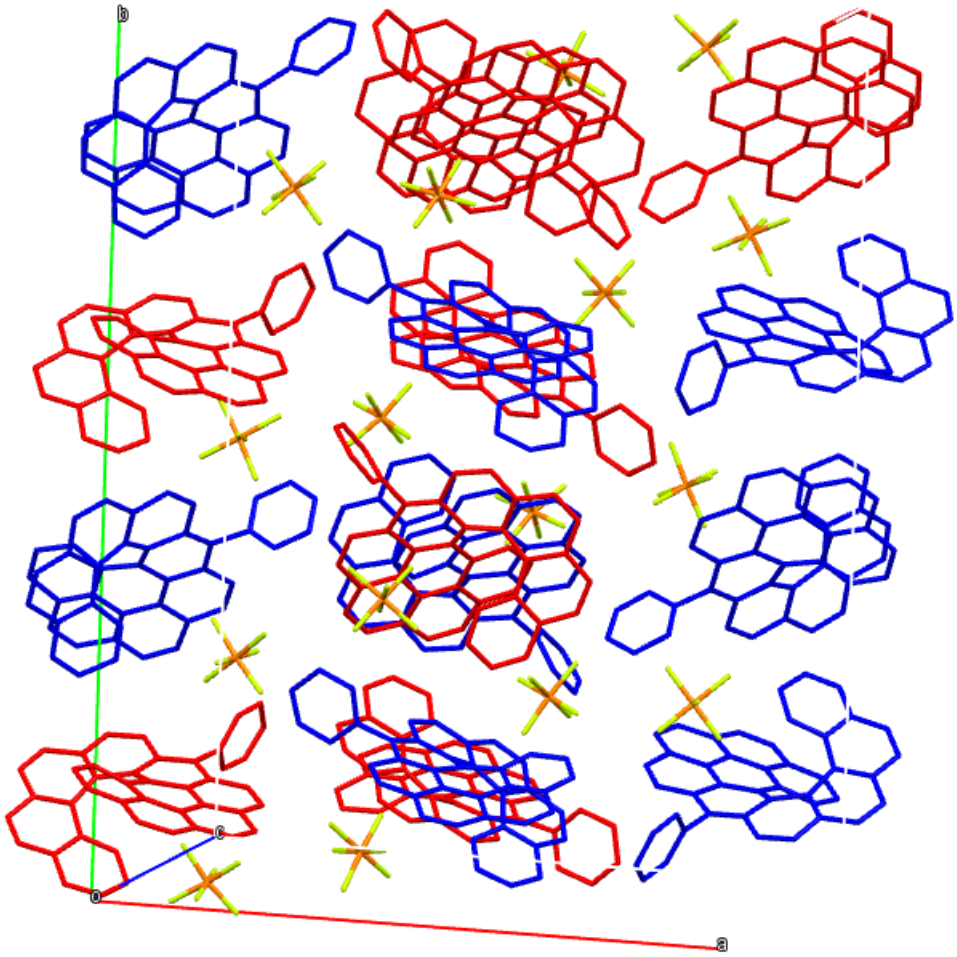

Figure S17. Molecular packing of the rac-**1**. *P* enantiomers are represented in blue and *M* enantiomers in red.

Table S3. Crystal data and structure refinement for rac-**1**.

Identification code	1
Empirical formula	$C_{43}H_{24}F_6NP$
Formula weight	6639.42
Temperature/K	130
Crystal system	orthorhombic
Space group	$Pna2_1$
a/Å	23.8345(6)
b/Å	32.6008(8)
c/Å	16.2939(4)
α/°	90
β/°	90
γ/°	90
Volume/Å^3	12660.7(5)
Z (Z')	16 (4)
ρ_{calc}g/cm^3	1.468
μ/mm^{-1}	1.339
F(000)	5728.0
Crystal size/mm^3	0.1 × 0.01 × 0.01
Radiation	CuKα (λ = 1.54178)
2Θ range for data collection/°	6.57 to 136.482
Reflections collected	63027
Independent reflections	18799 [R_{int} = 0.0576, R_{sigma} = 0.0628]
Data/restraints/parameters	18799/124/1837
Goodness-of-fit on F^2	1.037
Final R indexes [I>=2σ (I)]	R_1 = 0.1281, wR_2 = 0.2984
Final R indexes [all data]	R_1 = 0.1394, wR_2 = 0.3061

9. NMR spectra

N-phenyl-dibenzoacridinium (3)

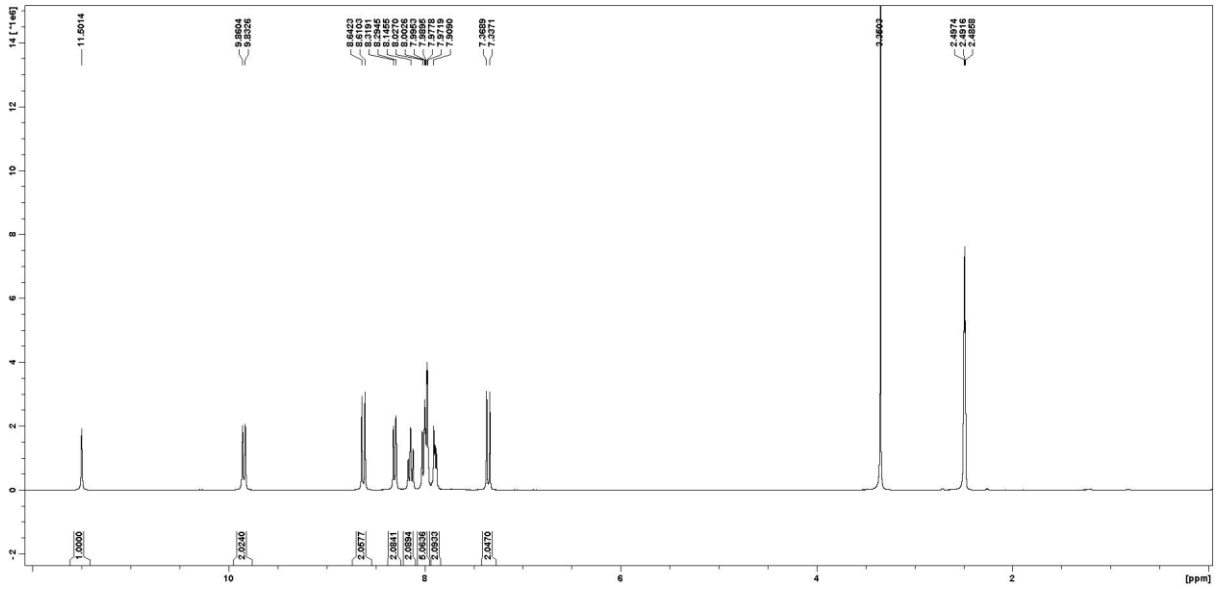

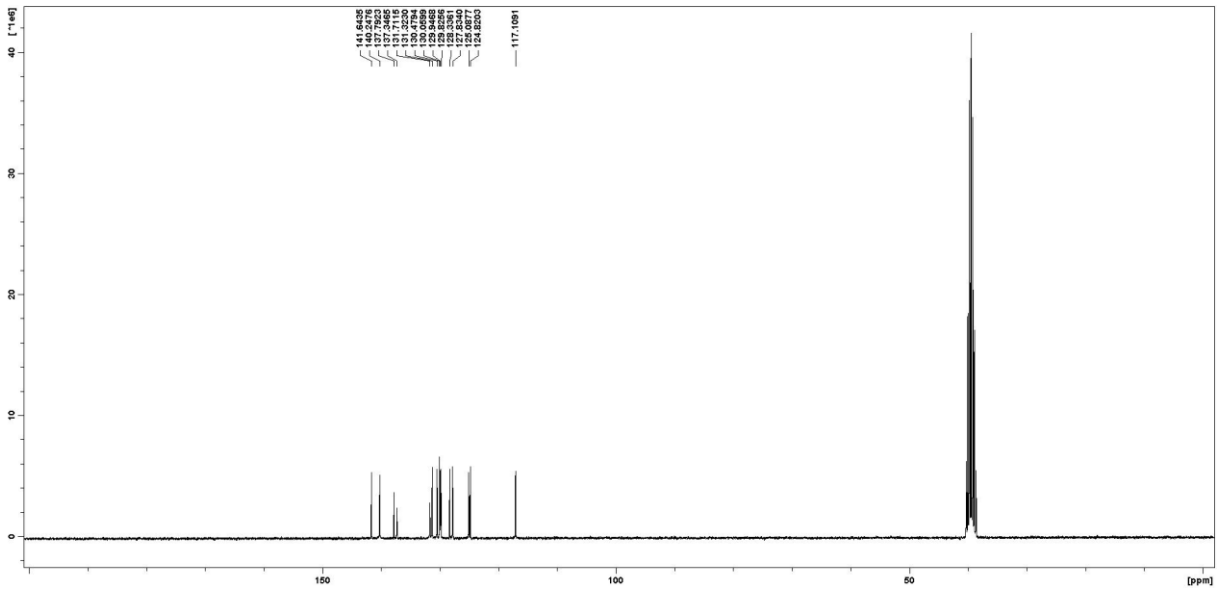

Triarylamine precursor (5)

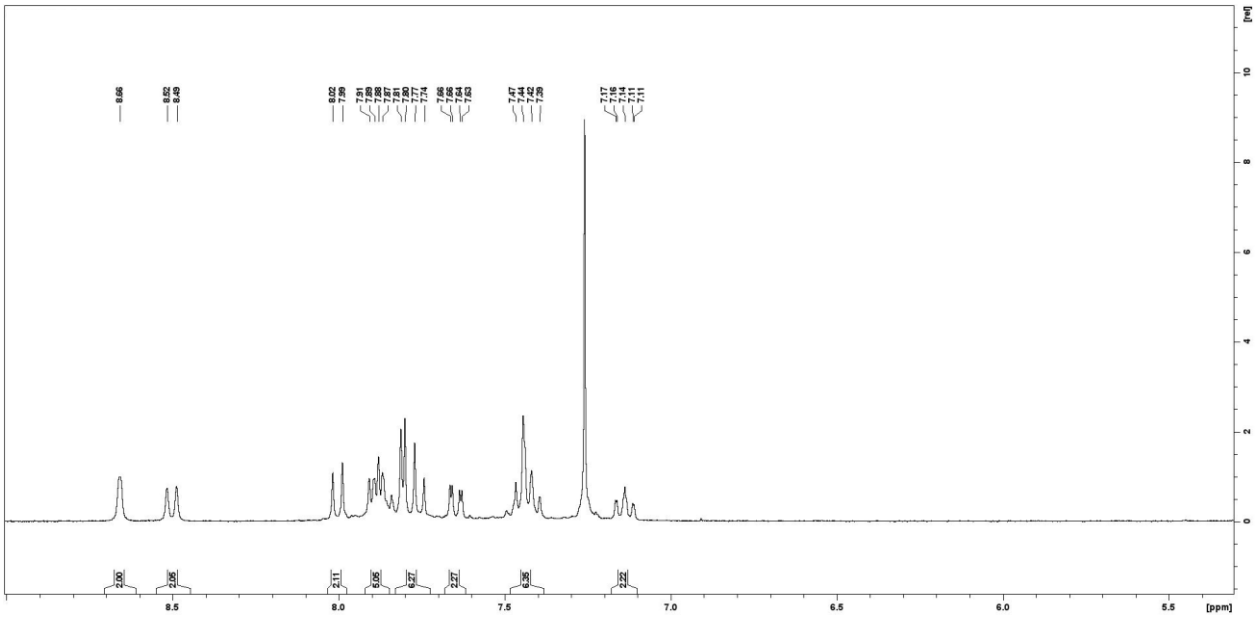

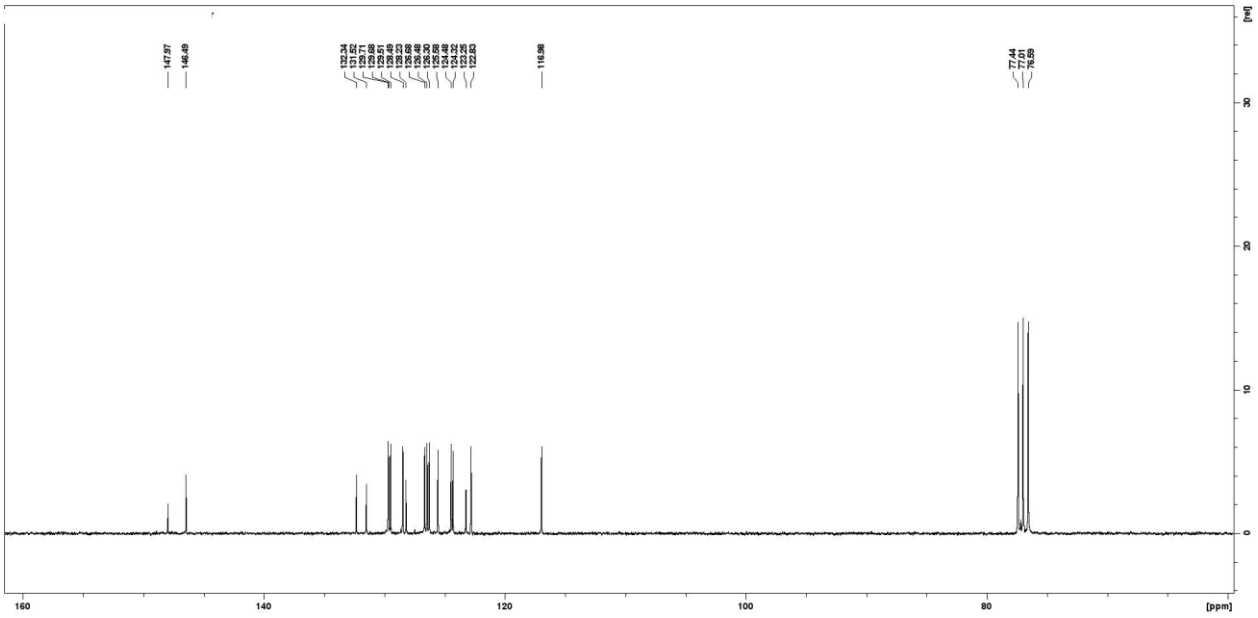

Aza-helicenium (1)